The Anrep effect requires transactivation of the epidermal growth factor receptor

María C. Villa-Abrille, Claudia I. Caldiz, Irene L. Ennis, Mariela B. Nolly, María J. Casarini, Gladys E. Chiappe de Cingolani, Horacio E. Cingolani and Néstor G. Pérez

Centro de Investigaciones Cardiovasculares, Facultad de Ciencias Médicas, Universidad Nacional de La Plata, Calle 60 y 120, 1900 La Plata, Argentina

Myocardial stretch elicits a biphasic contractile response: the Frank–Starling mechanism followed by the slow force response (SFR) or Anrep effect. In this study we hypothesized that the SFR depends on epidermal growth factor receptor (EGFR) transactivation after the myocardial stretch-induced angiotensin II (Ang II)/endothelin (ET) release. Experiments were performed in isolated cat papillary muscles stretched from 92 to 98% of the length at which maximal twitch force was developed (L_{max}). The SFR was $123 \pm 1\%$ of the immediate rapid phase ($n = 6$, $P < 0.05$) and was blunted by preventing EGFR transactivation with the Src-kinase inhibitor PP1 ($99 \pm 2\%$, $n = 4$), matrix metalloproteinase inhibitor MMPI ($108 \pm 4\%$, $n = 11$), the EGFR blocker AG1478 ($98 \pm 2\%$, $n = 6$) or the mitochondrial transition pore blocker clyclosporine ($99 \pm 3\%$, $n = 6$). Stretch increased ERK1/2 phosphorylation by $196 \pm 17\%$ of control ($n = 7$, $P < 0.05$), an effect that was prevented by PP1 ($124 \pm 22\%$, $n = 7$) and AG1478 ($131 \pm 17\%$, $n = 4$). In myocardial slices, Ang II (which enhances ET mRNA) or endothelin-1 (ET-1)-induced increase in O_2^- production ($146 \pm 14\%$, $n = 9$, and $191 \pm 17\%$, $n = 13$, of control, respectively, $P < 0.05$) was cancelled by AG1478 ($94 \pm 5\%$, $n = 12$, and $98 \pm 15\%$, $n = 8$, respectively) or PP1 ($100 \pm 4\%$, $n = 6$, and $99 \pm 8\%$, $n = 3$, respectively). EGF increased O_2^- production by $149 \pm 4\%$ of control ($n = 9$, $P < 0.05$), an effect cancelled by inhibiting NADPH oxidase with apocynin ($110 \pm 6\%$ $n = 7$), mKATP channels with 5-hydroxydecanoic acid (5-HD; $105 \pm 5\%$, $n = 8$), the respiratory chain with rotenone ($110 \pm 7\%$, $n = 7$) or the mitochondrial permeability transition pore with cyclosporine ($111 \pm 10\%$, $n = 6$). EGF increased ERK1/2 phosphorylation ($136 \pm 8\%$ of control, $n = 9$, $P < 0.05$), which was blunted by 5-HD ($97 \pm 5\%$, $n = 4$), suggesting that ERK1/2 activation is downstream of mitochondrial oxidative stress. Finally, stretch increased Ser703 Na$^+$/H$^+$ exchanger-1 (NHE-1) phosphorylation by $172 \pm 24\%$ of control ($n = 4$, $P < 0.05$), an effect that was cancelled by AG1478 ($94 \pm 17\%$, $n = 4$). In conclusion, our data show for the first time that EGFR transactivation is crucial in the chain of events leading to the Anrep effect.

Abbreviations Ang II, angiotensin II; ET, endothelin; EGF, epidermal growth factor; EGFR, epidermal growth factor receptor; GPCR, G protein coupled receptor; 5-HD, 5-hydroxydecanoic acid; L_{max}, the length at which maximal twitch force was developed; MMP, matrix metalloproteinase; MMPI, MMP inhibitor; MPTP, mitochondrial permeability transition pore; NCX, Na$^+$/Ca^{2+} exchanger; NHE-1, Na$^+$/H$^+$ exchanger-1; O_2^-, superoxide anion; PP1, Src-kinase inhibitor; ROS, reactive oxygen species; SFR, slow force response.

Introduction

In myocytes, angiotensin II (Ang II) is stored in secretory vesicles, and its release is triggered by mechanical stretch (Sadoshima *et al.* 1993; Leri *et al.* 1998). The release of Ang II is sufficient to activate angiotensin 1 (AT1) receptors in an autocrine/paracrine loop that leads to the release/formation of endothelin (ET) (Ito

et al. 1993; Yamazaki *et al.* 1996, 1998), the production of NADPH-dependent mitochondrial reactive oxygen species (ROS) (Zhou *et al.* 2006; Caldiz *et al.* 2007; Zhang *et al.* 2009), the activation of redox sensitive kinases, and the stimulation of the Na$^+$/H$^+$ exchanger-1 (NHE-1) (Akram *et al.* 2006; Caldiz *et al.* 2007). One consequence of this chain of events appears to be myocardial hypertrophy (Ennis *et al.* 2007).

In concert with the autocrine/paracrine loop, myocardial stretch triggers an increase in cardiac contractility that develops immediately after the Frank–Starling mechanism, reaching a maximum after 10 to 15 min. This is due to an increase in the intracellular calcium transient, without changes in myofilament calcium sensitivity (Allen & Kurihara, 1982; Kentish & Wrzosek, 1998; Perez *et al.* 2001). This mechanical counterpart of the autocrine/paracrine loop is called the slow force response to stretch (SFR) (Parmley & Chuck, 1973; Calaghan & White, 2001) or the Anrep effect (von Anrep, 1912; Sarnoff *et al.* 1960; Alvarez *et al.* 1999). The SFR seems to involve the early intracellular signals that lead to myocardial hypertrophy; in particular, mitochondrial ROS formation seems to be crucial (Caldiz *et al.* 2007; Zhang *et al.* 2009). Interestingly, recent evidence suggested that Ang II, the first step in the chain of events that leads to SFR, requires the transactivation of endothelial growth factor receptor (EGFR) to induce cardiac hypertrophy (Kagiyama *et al.* 2002; Zhai *et al.* 2006; Szokodi *et al.* 2008). Furthermore, in neonatal cardiac myocytes, stretch elicited a mechanism that required EGFR transactivation to induce the release/formation of ET and, consequently, the activation of extracellular signal-regulated kinase (ERK) (Asakura *et al.* 2002; Duquesnes *et al.* 2009). We therefore hypothesised that transactivation of the EGFR must be critical for the development of the SFR.

This study investigated whether blunting the G protein coupled receptor (GPCR)-mediated transactivation of EGFR would block the SFR. A preliminary report of our data has been presented elsewhere (Perez *et al.* 2009).

Methods

All procedures followed during this investigation conform to the *Guide for the Care and Use of Laboratory Animals* published by the US National Institutes of Health (NIH Publication No. 85-23, revised 1996), to the guidelines laid down by the Animal Welfare Committee of the La Plata School of Medicine, and the policies of *The Journal of Physiology* (Drummond, 2009). Cats ($n = 42$, body weight 3–4 kg) were anaesthetized by intraperitoneal injection of sodium pentobarbitone (35 mg (kg body weight)$^{-1}$). The chests were opened to excise the heart when deep anaesthesia was reached, verified by the loss of corneal reflex and appearance of slow deep diaphragmatic breathing. Animals were provided by a local supplier (San Cayetano, Monte Grande, Argentina). Each heart was used to provide papillary muscles as well as cardiac tissue slices.

Isolation of papillary muscles

Papillary muscles from the right ventricle were used to assess the SFR to stretch as previously described (Perez *et al.* 2001). Briefly, the muscles were mounted in a perfusion chamber placed on the stage of an inverted microscope (Olympus) and superfused at a constant rate (5 ml min^{-1}) with a $CO_2/HCO_3{}^-$-buffered solution containing (mmol l^{-1}): NaCl 128.3, KCl 4.5, $CaCl_2$ 1.35, $NaHCO_3$ 20.23, $MgSO_4$ 1.05, glucose 11.0 and equilibrated with 5% CO_2–95% O_2 (pH ~7.40). The possible participation of catecholamines released by the nerve endings was prevented by adrenergic receptors blockade with 1.0 μmol l^{-1} prazosin plus 1.0 μmol l^{-1} atenolol. The muscles were paced at 0.2 Hz at a voltage 10% over threshold maintained at 30°C, and isometric contractions were recorded. Cross sectional area (calculated as 0.75 of the product of thickness and width) was used to normalize force records obtained with a silicon strain gauge (model AEM 801, Sensonor Technologies, Horten, Norway). The slack length of each muscle was determined after mounting, and then the muscles were progressively stretched to the length at which they developed maximal twitch force (L_{max}). After a few minutes at L_{max}, they were shortened to obtain the 95% of the maximal twitch force (length that approximated 98% of L_{max} and referred to as L_{98}). Then, the muscles were shortened to 92% of L_{max} (L_{92}) and maintained at this length until the beginning of the experimental protocol, when they were abruptly stretched from L_{92} to L_{98}. The drugs were added to the perfusate 20 min before stretch, and during this period, none of them changed the developed force by more than 3% to 4%.

Cardiac tissue slices

Preparation of cardiac slices. Hearts were quickly removed from previously anaesthetized animals. The hearts were perfused through the aorta with Krebs–Ringer buffer pH 7.4 to eliminate the blood, and tissue slices from the left ventricle (1 × 5 mm) were cut and kept at 4°C until assayed. Assay buffer consisted of Krebs-Hepes buffer of the following composition (in mmol l^{-1}): 118.3 NaCl; 4.7 KCl; 1.8 $CaCl_2$; 1.2 $MgSO_4$; 1.0 K_2HPO_4; 25 $NaHCO_3$; 11 glucose; 20 Hepes (pH 7.4 after 1.5 h aeration with 95% O_2–5% CO_2 at 37°C). Cardiac tissues were incubated in assay buffer during 30 min in the presence of different drugs in a metabolic incubator under 95% O_2–5% CO_2 at 37°C before measurements of $O_2{}^-$ production.

Measurements of superoxide anions ($\cdot O_2{}^-$) production. We used lucigenin-enhanced chemiluminescence to measure $O_2{}^-$ production by cat cardiac tissue in Krebs-Hepes buffer with 5 μmol l^{-1} lucigenin as described previously (Caldiz *et al.* 2007). The chemiluminescence in arbitrary units (AU) was recorded with a luminometer (Chameleon; Hidex, Turku, Finland) during 30 s, each with a 4.5 min interval during 30 min. $O_2{}^-$ production was

normalized to milligrams dry weight tissue per minute. Control tissue slices without any pharmacological intervention produced low levels of O_2^- that were only slightly above background. Although the lucigenin-enhanced chemiluminescence method does not allow accurate detection of the basal O_2^- production (Dikalov *et al.* 2007), its sensitivity was enough to detect an increase in O_2^- production above background after Ang II, ET-1 and EGF. When necessary, the increase in O_2^- production was expressed as a percentage of basal value after 15 min of each intervention.

Determination of extracellular signal-regulated protein kinases (ERK1/2) and NHE-1 phosphorylation

Cardiac tissue was homogenized in lysis buffer ($300 \ mmol \ l^{-1}$ sucrose; $1 \ mmol \ l^{-1}$ dithiothreitol (DTT); $4 \ mmol \ l^{-1}$ EGTA, protease inhibitor cocktail (Complete Mini, Roche); $20 \ mmol \ l^{-1}$ Tris-HCl, pH 7.4). After a brief centrifugation the supernatant was kept and protein concentration determined by the Bradford method. Samples were denatured and equal amounts of protein were subjected to PAGE and electro-transferred to PVDF membranes. Membranes were then blocked with non-fat dry milk and incubated overnight with either anti-phospho-ERK1/2 or anti-ERK 2 (Santa Cruz Biotechnology, Santa Cruz, CA, USA). For NHE-1 phosphorylation determination, samples were immunoprecipitated using a NHE-1 polyclonal antibody (Chemicon, Temecula, CA, USA) and then subjected to PAGE, electrotransferred and incubated with an anti-14-3-3 binding motif antibody (Cell Signaling Technology, Inc., Danvers, MA, USA). Previous reports have shown that the regulatory Ser703 of the NHE-1 lies within a sequence which creates upon phosphorylation a binding motif for 14-3-3 proteins (Takahashi *et al.* 1999; Lehoux *et al.* 2001). Thus, the anti-P-14-3-3 binding motif antibody when probed with immuno-precipitated NHE-1 represents a useful tool to estimate NHE-1 phosphorylation at Ser703 (Snabaitis *et al.* 2006). Total ERK-2 and NHE-1 as a loading control were assayed. Peroxidase-conjugated anti-rabbit or anti-mouse IgG (Santa Cruz Biotechnology) was used as secondary antibody and bands were visualized using the ECL-Plus chemiluminescence detection system (GE Healthcare, Little Chalfont, UK). Autoradiograms were analysed by densitometric analysis (Scion Image).

RNA measurements by RT-PCR

Total RNA was isolated from the cardiomyocytes suspension using the RNeasy kit (Qiagen, Valencia, CA, USA) according to the manufacturer's instructions. RNA ($0.8 \ \mu g$) was reverse-transcribed using the Omniscript RT

kit (Qiagen). A dilution of the resulting cDNA was used for quantifying the relative content of mRNA by real-time PCR (iCycler iQ Real-Time PCR Detection System, Bio-Rad) using appropriate primers and SYBR Green as a fluorescent probe. The following primers, designed using Primer3 software, were used: GAPDH: forward primer 5-GGGTGTGAACCACGAGAAAT-3; reverse primer 5-CCACAGTCTTCTGAGTGGCA-3; preproET-1: forward primer 5-CAGACAAAGAACTCCGAGCC-3; reverse primer 5-GGTCTTGATGCTGTTGCTGA-3. PCR reactions were performed with TaqDNA polymerase (Invitrogen). Fluorescence data were acquired at the end of extension. A melt analysis was run for all of the products to determine the specificity of the amplification. The cycle threshold values for each gene were measured and calculated by computer software (iCycler IQ OSS, version 3.0a, Bio-Rad). The cycle threshold values for each gene were normalized by those GAPDH in the same sample. The primers were designed against the feline sequences. For each experiment of real-time RT-PCR we obtained a melting curve of the amplified gene where it could be appreciated that only a specific product was amplified in each case with no primer-dimer formation.

Statistics

Results are expressed as means $\pm$ S.E.M. Differences between initial phase and post-stretch records, comparison of O_2^- production after 15 min of incubation with the different drugs and ERK1/2 phosphorylation under the different conditions were assessed by one-way ANOVA followed by the Student–Newman–Keuls test. Two-way ANOVA was used to compare post-stretch data in the absence and presence of drugs. $P < 0.05$ was considered significant.

Results

Probing the intracellular signalling pathway triggered by myocardial stretch

Figure 1*A* shows a typical force response to stretch when an isolated cat papillary muscle is stretched from 92 to 98% of its maximum length. The result is a biphasic contractile response: the classical Frank–Starling mechanism is manifested immediately after stretch, followed by a gradually developing increase in force, known as the SFR to stretch or the Anrep effect.

Previous studies from our and other laboratories have provided evidence that the SFR is the result of an autocrine/paracrine loop that begins with the activation of GPCRs (Ang II and ET) and ends with an increase in the Ca^{2+} transient through the Na^+/Ca^{2+} exchanger (Cingolani *et al.* 1998; Yamazaki *et al.* 1998; Alvarez *et al.*

1999; Calaghan & White, 2001; Perez *et al.* 2001, 2003; Luers *et al.* 2005). The role of mitochondrial ROS in the intracellular signalling pathway was also recently described (Caldiz *et al.* 2007; Zhang *et al.* 2009).

In order to probe the connection between EGFR transactivation and the SFR, we explored whether inhibiting EGFR transactivation would affect the SFR of a papillary muscle. Several mediators are known to be involved in the transactivation process, but the precise communication between the GPCR and EGFR is not entirely understood (Wetzker & Bohmer, 2003). One proposed mediator is Src tyrosine kinase (Wetzker & Bohmer, 2003); thus, as a first test of our hypothesis, we inhibited Src kinase with the specific tyrosine kinase inhibitor PP1. Figure 1*C* shows that PP1 ($1 \mu mol\, l^{-1}$) completely cancelled the SFR to stretch. Another proposed mediator (Krieg *et al.* 2004; Szokodi *et al.* 2008) of EGFR transactivation was heparin-binding EGF (HB-EGF). HB-EGF is generated through extracellular proteolytic cleavage of proHB-EGF by the action of a matrix metalloproteinase (MMP). To test the contribution of this signalling pathway to the SFR, we inhibited MMP with MMP inhibitor III (MMPI), which specifically targeted MMPs 1, 2, 3, 7 and 13. MMPI ($3 \mu mol\, l^{-1}$) did not completely eliminate the SFR, but significantly reduced its magnitude by ~60% (Fig. 1*B*). This provided further support of the notion that EGFR transactivation was required for a fully developed SFR.

Finally, we specifically inhibited the EGFR with AG1478 ($1 \mu mol\, l^{-1}$), which is known to prevent receptor phosphorylation, and consequently, blocks receptor activation. Under these conditions, the SFR was completely abolished (Fig. 1*D*). The average SFR observed under the different experimental conditions was expressed as a percentage of the initial rapid phase (Fig. 1*E*).

Thus, these three interventions that interfered with the mechanism of transactivation significantly decreased the SFR. These results support the hypothesis that EGFR transactivation plays a role in the development of the SFR in cat myocardium.

Activation of redox sensitive kinases after myocardial stretch

We (Cingolani *et al.* 2005; Caldiz *et al.* 2007) and others (Zhang *et al.* 2009) have previously shown that the SFR depends on the activation of NHE-1, which is a target of the redox sensitive kinases, ERK1/2. Others showed that ROS stimulated NHE-1 through MAPK (Rothstein *et al.* 2002; Haworth *et al.* 2003; Fliegel & Karmazyn, 2004; Akram *et al.* 2006), and we recently proposed that stretch induced the mitochondrial production of ROS (Caldiz *et al.* 2007).

In this study, muscles were frozen 5 min after myocardial stretch and processed for kinase detection. We detected a significant increase in ERK1/2 phosphorylation. This effect was cancelled by pre-treatment with either AG1478 or PP1 (Fig. 2), two inhibitors of EGFR transactivation that also blocked the mechanical response. These findings showed that the prevention of EGFR phosphorylation and activation is able to cancel both the increase in ERK1/2 phosphorylation and the mechanical response to stretch.
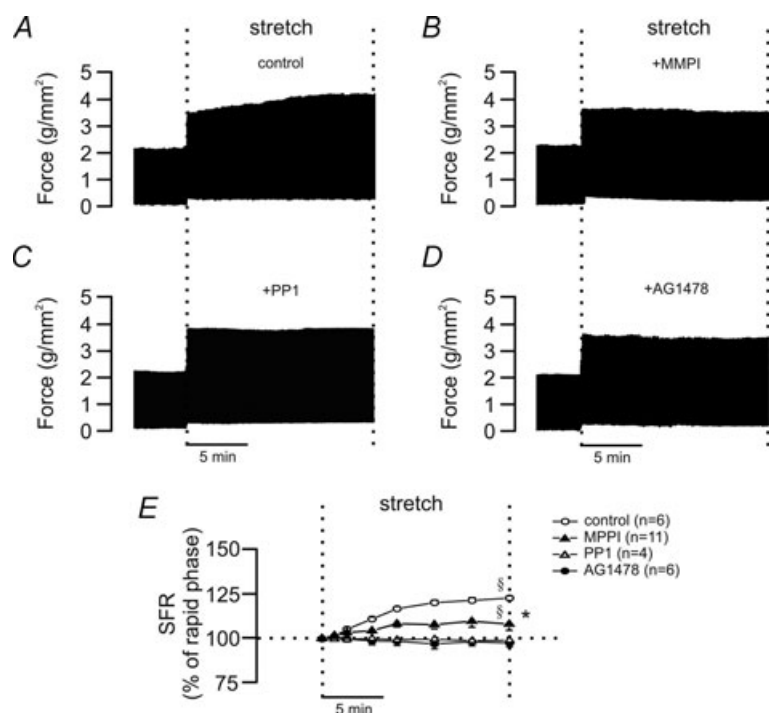

Figure 1. SFR and EGFR transactivation
A, a typical force record from a cat papillary muscle subjected to an increase in length from 92 to 98% of L_{max}; the biphasic response to stretch can be seen (vertical dotted lines indicate stretching interval). *B–D*, same as *A* but from muscles pretreated with matrix metalloproteinase inhibitor (MMPI, *B*), the Src kinase inhibitor PP1 (*C*) or the EGFR blocker AG1478 (*D*), interventions that cancel EGFR transactivation. As can be seen, all these pharmacological interventions prevented the development of the SFR to stretch. *E*, the averaged results obtained under the different experimental conditions expressed as a percentage of the initial rapid phase. *$P < 0.05$ control curve *vs.* others (2-way ANOVA). §$P < 0.05$ *vs.* initial rapid phase (for the sake of clarity, significance is indicated only for 15 min of stretch).

Ang II, ET-1, ROS production and transactivation of the EGFR

We proposed that mitochondrial ROS are a necessary upstream signal for ERK1/2 activation, NHE-1 phosphorylation, and SFR development. Our proposal was based on evidence that physiological concentrations of exogenous Ang II or ET-1 induced a NADPH-dependent increase in O_2^- formation, and this could be blunted by interfering with the mitochondrial ROS source (Caldiz *et al.* 2007). Here, we found that either AG1478 or PP1 suppressed Ang II/ET-1-induced O_2^- formation in cat myocardial slices (Fig. 3). These results implied that EGFR transactivation is critical in mediating the Ang II and ET-1 induction of ROS production.

Ang II–ET-1 cross talk

Myocardial stretch causes the release of preformed Ang II from neonatal (Sadoshima *et al.* 1993) and adult myocytes (Leri *et al.* 1998). The effects induced by physiological Ang II concentrations can be blunted by interfering with ET-1, either by blocking the endothelin type-A (ETA) receptor or by inhibiting the ET conversion enzyme (Alvarez *et al.* 1999; Perez *et al.* 2001; Cingolani *et al.* 2005, 2006). Furthermore, the presence of prepro-ET, Big ET, and ET was detected in the cardiomyocytes (Cingolani *et al.* 2006). Therefore, myocardial stretch induces Ang II and/or ET actions.

The mechanism by which Ang II elicited ET release/formation is not fully known. Based on studies on B-type natriuretic peptide production in neonates, Anderson *et al.* (2004) proposed that stretch induced ET release through a NADPH-dependent, redox-sensitive mechanism. Consistent with his proposal, we found that $1\,\mathrm{nmol\,l^{-1}}$ of Ang II increased the mRNA expression of ET-1 in cat myocytes (Fig. 4), perhaps reflecting the replenishment of a released pool and/or increased ET-1 formation. This effect was inhibited by the AT1 blocker losartan, the NADPH inhibitor apocynin and the ROS scavenger 2-mercaptopropionyl glycine. The exact mechanism of the cross talk between Ang II and ET-1 is out of the scope of this study; however, these findings showed that the cross talk between Ang II and ET-1 was sensitive to the redox state in the adult feline heart.

Increased ROS formation by EGF signalling

In order to investigate this mechanism further, we evaluated whether EGF was able to increase O_2^- formation under our experimental conditions. We found that EGF increased myocardial O_2^- production in a dose-dependent manner (Fig. 5). The effect of EGF at $0.1\,\mu\mathrm{g\,ml^{-1}}$ was similar to the increase in O_2^- production observed with $1\,\mathrm{nmol\,l^{-1}}$ ET-1; thus, we decided to use this EGF concentration in the following experiments. The increase in O_2^- production induced by $0.1\,\mu\mathrm{g\,ml^{-1}}$ EGF was, as expected, cancelled by pre-treatment with the EGFR
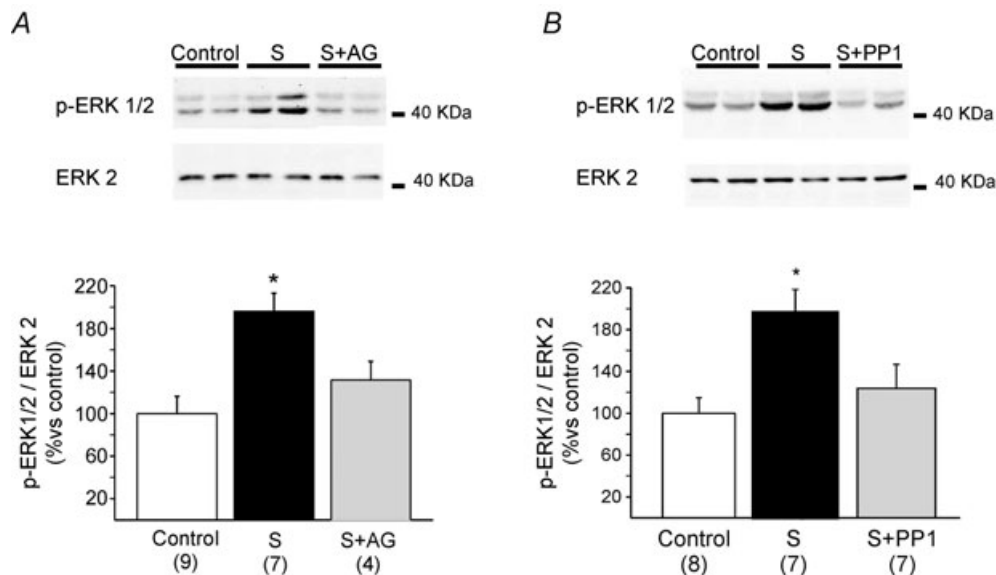

Figure 2. ERK1/2 phosphorylation after stretch
Five minutes of stretch significantly increased ERK1/2 phosphorylation, kinases upstream NHE-1, that we have previously shown to play a critical role in SFR development (Caldiz *et al.* 2007). This effect was blunted either by EGFR blockade with AG1478 (AG, *A*) or by Src kinase inhibition with PP1 (*B*), demonstrating that EGFR transactivation after stretch is necessary for ERK1/2 phosphorylation. It is important to highlight that either AG1478 or PP1 alone did not modify basal ERK1/2 phosphorylation ($92 \pm 4\%$, $n = 4$, and $107 \pm 8\%$, $n = 4$, of control respectively). *$P < 0.05$ *vs.* non-stretched control.

blocker AG1478, but not by the Src kinase inhibitor PP1 (Fig. 5B), which is upstream of the EGFR transactivation pathway (Wetzker & Bohmer, 2003; Krieg *et al.* 2004). As reported previously for Ang II/ET-1 (Caldiz *et al.* 2007), the increase in ROS production was NADPH dependent, since it was eliminated by apocynin (Fig. 5B). Furthermore, EGF-induced ROS production was abrogated by blocking mitochondrial ATP-sensitive potassium channels (mKATP) with 5-hydroxydecanoic acid (5-HD; a mKATP-specific blocker) and glybenclamide (a non-selective KATP blocker), or the mitochondrial respiration inhibitor rotenone (Fig. 5B). Thus, these data support the notion that Ang II elicits an increase in mitochondrial ROS formation through an intracellular signalling pathway that involves ET and EGFR transactivation.

ERK1/2 phosphorylation by EGF: role of mitochondria

Next, we reasoned that, if Ang II/ET-1 generated the ROS that activated the ERK1/2 kinases and led to
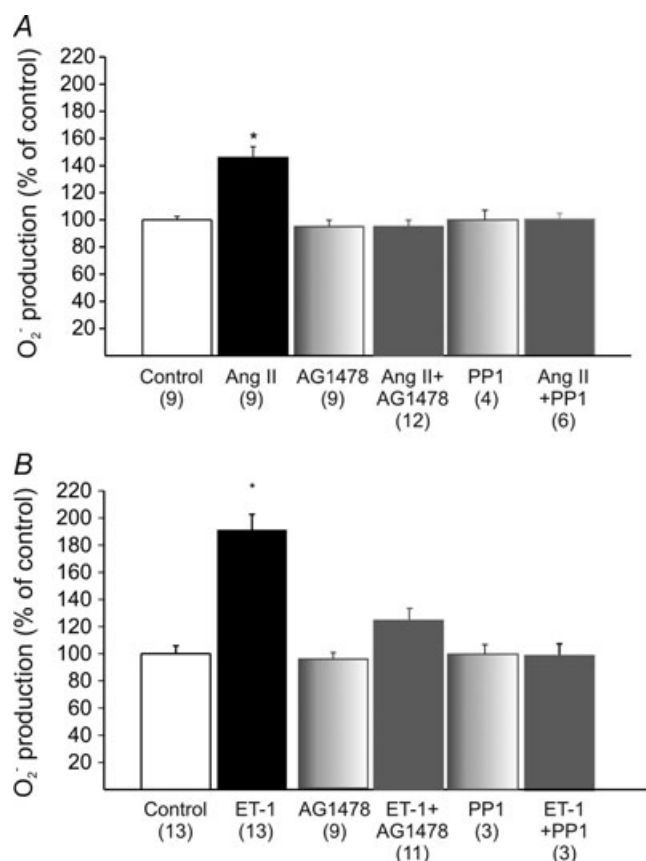
Figure 3. O$_2^-$ production after addition of Ang II or ET-1 in cardiac slices
The increase in O$_2^-$ production induced either by 1 nmol l^{-1} Ang II (*A*) or 1 nmol l^{-1} ET-1 (*B*) was cancelled by AG1478 or PP1. These findings demonstrate that the well known increase in ROS production after Ang II/ET-1 treatment requires EGFR transactivation in the myocardium. *$P < 0.05$ *vs.* control.

NHE-1 phosphorylation (Rothstein *et al.* 2002; Haworth *et al.* 2003; Fliegel & Karmazyn, 2004; Caldiz *et al.* 2007), and these effects depended on EGFR transactivation, then EGF should be able to induce ERK1/2 phosphorylation. Figure 6 shows that an increase in ERK1/2 phosphorylation was induced by 0.1 µg ml^{-1} EGF. This increase was abolished by AG1478 (not shown), and also by inhibiting the NADPH oxidase (apocynin), the mKATP channels (with 5-HD or glybenclamide) or the mitochondrial respiratory chain (rotenone). This clearly suggested that mitochondrial ROS formation was a necessary step upstream of ERK 1/2 phosphorylation.

Role of mitochondrial permeability transition pore (MPTP) in SFR

Based on the above data, we could conclude that SFR development depended on EGFR transactivation inducing the formation of mitochondrial ROS. Transactivation may induce mitochondrial ROS formation by promoting the opening of mKATP channels. This would, in turn, modulate MPTP formation and lead to an increase in O$_2^-$ production. If the MPTP were involved in mitochondrial ROS release, then the prevention of MPTP opening should prevent ROS formation and thus block the SFR to stretch. Figure 7 shows that this was indeed the case. Pretreatment of papillary muscles with the MPTP inhibitor cyclosporine A (0.5 µmol l^{-1}) completely cancelled the SFR.
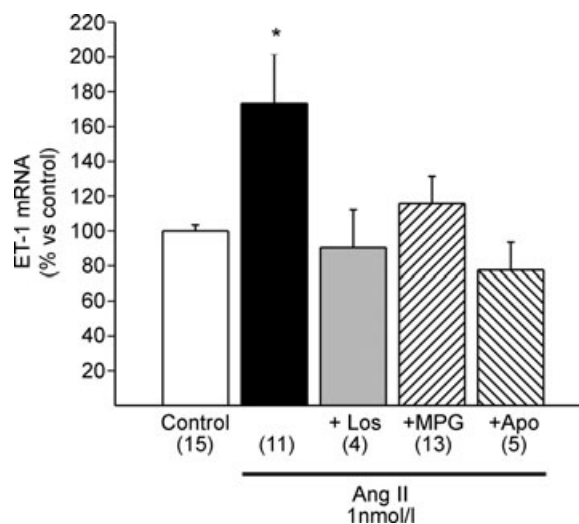
Figure 4. Ang II–ET-1 crosstalk
Ang II (1 nmol l^{-1}) promoted a significant increase in preproET-1 mRNA expression detected by real-time RT-PCR, a result that confirms the Ang II–ET crosstalk in the cat myocardium. This increase in preproET-1 mRNA was, as expected, not only cancelled by AT1 receptor blockade with losartan (Los), but also by scavenging ROS with 2-mercaptopropionyl glycine (MPG) or by inhibiting NADPH oxidase with apocynin (Apo), indicating that NADPH oxidase-mediated ROS production is a key step to increase ET-1 expression. *$P < 0.05$ *vs.* control.
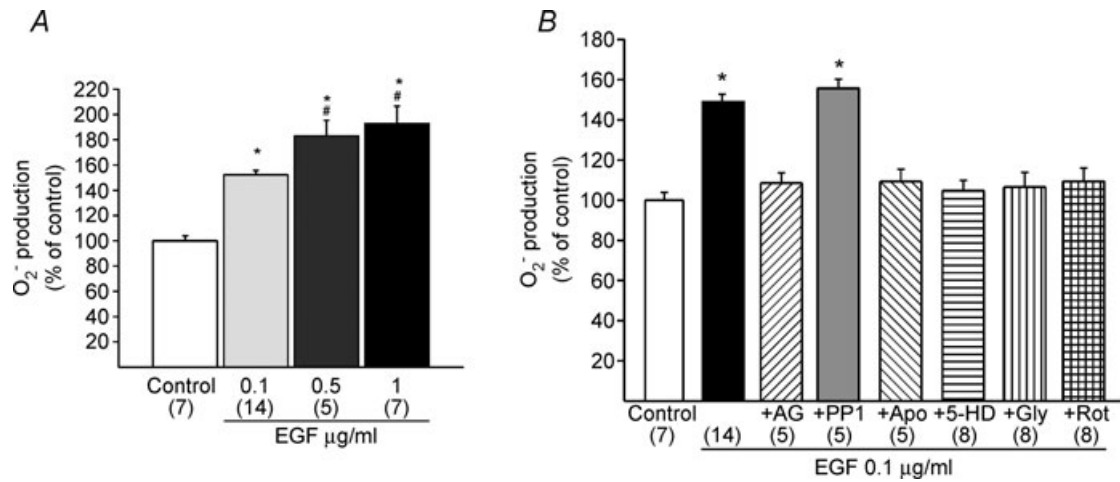
Figure 5. O_2^- production after addition of EGF in cardiac slices
Direct activation of the EGFR by EGF significantly enhanced O_2^- production in a dose-dependent manner (*A*). We selected the lower concentration of EGF (0.1 μg ml^{-1}) to perform subsequent experiments because it increased O_2^- production in a similar magnitude to 1 nmol l^{-1} ET-1 (see Fig. 3). As expected, the 0.1 μg ml^{-1} EGF effect was blunted by specific EGFR blockade with AG1478 (AG) but not by Src kinase inhibition with PP1 (*B*) since the latter is located upstream of EGFR. The EGF-induced increase in O_2^- production was also prevented by NADPH oxidase inhibition with apocynin (Apo), by two different mitochondrial ATP-sensitive K$^+$ channel (mKATP) blockers (5-hydroxydecanoate (5-HD) and glybenclamide (Gly)), and also by the respiratory chain inhibitor rotenone (Rot). These data support the hypothesis that EGF is a necessary mediator in the stretch-induced mitochondrial ROS production. * and # indicate $P < 0.05$ *vs.* control and 0.1 μg ml^{-1} EGF respectively.

In addition, cyclosporine prevented the EGF-mediated increase in O_2^- production (Fig. 7).

The changes in O_2^- production were measured by the lucigenin method; thus, we could not determine whether the activation of kinases and NHE was mediated by O_2^- or H_2O_2. O_2^- is very unstable, and it is rapidly converted by superoxide dismutase (SOD) into H_2O_2, a more stable, membrane-permeant ROS that is widely recognized as a signalling molecule. In the myocardium, dismutation is performed by a membrane bound extracellular SOD, a cytoplasmic CuZn SOD, and a mitochondrial Mn SOD. Therefore, the O_2^- detected in cardiac slices might be easily converted into H_2O_2 at different cellular locations, upstream or downstream of the mitochondria. Furthermore, Sabri *et al.* (1998) and Rothstein *et al.* (2002) demonstrated that H_2O_2 was the intracellular signal that led to the activation of kinases that phosphorylated the NHE; furthermore, we have previously shown that promoting an increased conversion of O_2^- into H_2O_2 led to an enhanced SFR (Caldiz *et al.* 2007). These results suggested that H_2O_2 plays an important role in the development of the SFR or Anrep effect.

NHE-1 phosphorylation

We (Cingolani *et al.* 1998; Alvarez *et al.* 1999; Cingolani *et al.* 2005) and others (Calaghan & White, 2001; Luers *et al.* 2005) have previously demonstrated that the SFR was cancelled by NHE-1 inhibitors in different species. The

underlying mechanism was the prevention of the NHE-1 activation-induced increase in intracellular Na$^+$ that would favour intracellular Ca^{2+} accumulation through the
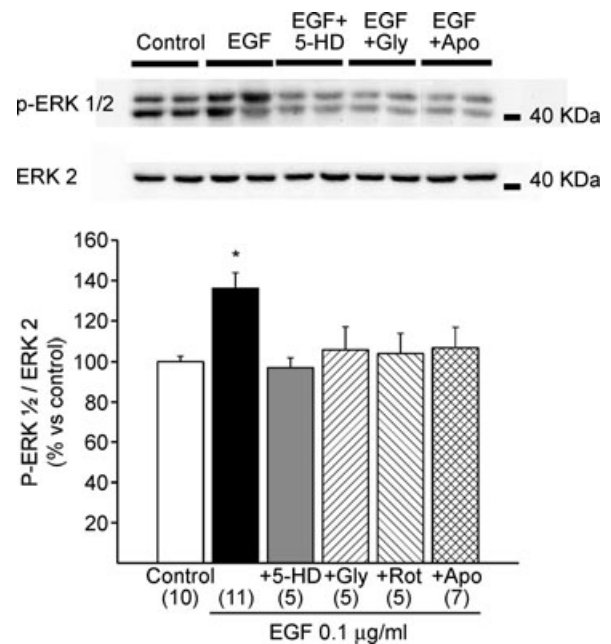

Figure 6. ERK1/2 phosphorylation after EGF stimulation
EGF significantly increased ERK1/2 phosphorylation, an effect that was cancelled by 5-HD, glybenclamide (Gly), rotenone (Rot) or apocynin (Apo). These results further support the notion that mitochondrial ROS formation is a necessary upstream step to ERK 1/2 phosphorylation. *$P < 0.05$ *vs.* control.

Na^+/Ca^{2+} exchanger (Alvarez *et al.* 1999; Perez *et al.* 2001, 2003).

Previous reports (Takahashi *et al.* 1999; Lehoux *et al.* 2001; Snabaitis *et al.* 2006) have shown that Ser703 in the regulatory carboxyl-tail of NHE-1 creates a binding motif for 14-3-3 proteins upon phosphorylation by ERK1/2-p90RSK cascade. We estimated the levels of NHE-1 phosphorylation at Ser703 with a phospho-Ser 14-3-3 binding motif antibody. Figure 8 shows that phosphorylation in the 14-3-3 binding motif was increased with myocardial stretch and the increase was prevented with AG1478. A limitation of our study is that NHE-1

phosphorylation was estimated by an antibody that specifically detects P-Ser703; potential changes in the phosphorylation state of other sites of the exchanger, which might contribute to the SFR, were not explored in the present work.

Our results support the notion that GPCR induced-EGFR transactivation plays a role in the chain of events that lead to NHE-1 phosphorylation and SFR development.

Discussion

In 1912, von Anrep (von Anrep, 1912) observed that, when aortic resistance was elevated, ventricular volume first increased and then declined towards its original value. An influence appeared to operate soon after the initial dilatation, which caused the heart to return toward the control volume. Rosenblueth *et al.* (1959) made similar observations in the right ventricle. Sarnoff *et al.* (1960) coined the expression 'homeometric autoregulation' to denote a mechanism that countered changes in myocardial length (Frank–Starling mechanism or heterometric auto-regulation) and originated in the same myocardium.
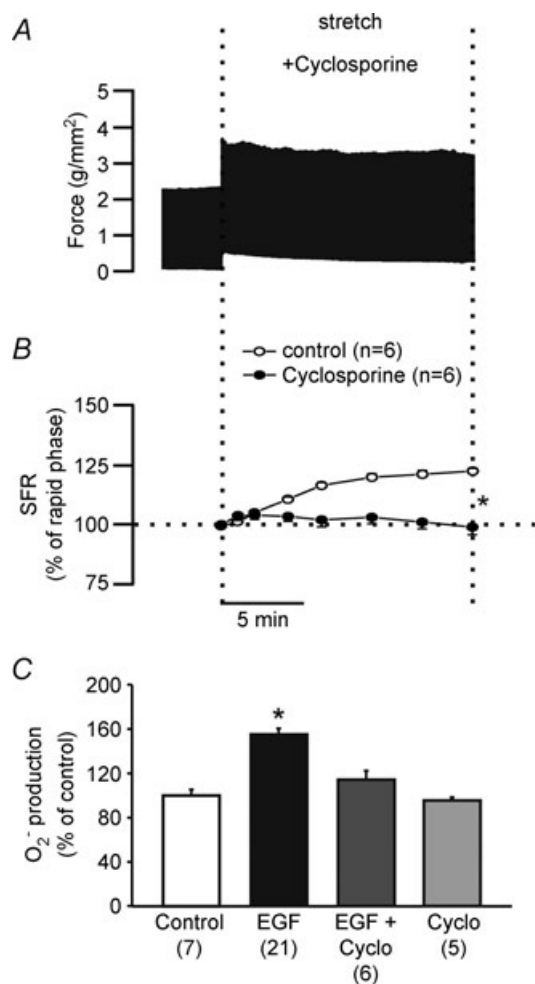

Figure 7. Role of MPTP in the development of the SFR
MPTP inhibition with cyclosporine cancelled the SFR as shown in *A* (representative force record) and B (averaged results expressed as a percentage of the initial rapid phase). Interestingly, cyclosporine also cancelled the increase in O_2^- production induced by 0.1 ng ml^{-1} EGF. These results suggest a role for MPTP in the development of the Anrep effect, probably by permitting the release of mitochondrial ROS. For the sake of comparison a control SFR already presented in Fig. 1*E* and a control EGF-promoted O_2^- production shown in Fig. 5*B* were also included in panels *B* and *C*. *$P < 0.05$ *vs.* control (panel *B*) or *vs.* EGF (panel *C*).
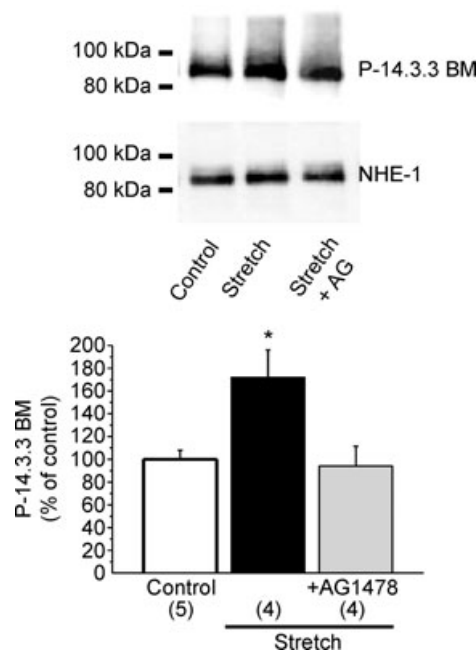

Figure 8. Stretch-induced NHE-1 phosphorylation
Five minutes of stretch significantly increased NHE-1 phosphorylation at Ser703 estimated by a phospho-Ser 14-3-3 binding motif antibody. This effect was cancelled when the EGFR was blocked by AG 1478 (AG). These results support a role of the EGFR transactivation in the chain of events leading to NHE-1 phosphorylation and SFR development. It is important to highlight that AG1478 alone did not modify basal NHE-1 phosphorylation ($93 \pm 4\%$ of control, $n = 4$). *$P < 0.05$ *vs.* control.

In 1973, Parmley and Chuck reproduced this phenomenon in myocardial strips (Parmley & Chuck, 1973). They excluded the possibility that changes in coronary blood flow could be responsible for the phenomenon (Monroe *et al.* 1972). Subsequently, other investigators (Allen & Kurihara, 1982; Kentish & Wrzosek, 1998; Alvarez *et al.* 1999; Calaghan & White, 2001; Perez *et al.* 2001) provided further insight on the mechanisms involved in the increase in myocardial force triggered by myocardial stretching.

In our laboratory, the finding that myocardial stretch induced alkalization in cat papillary muscles bathed in bicarbonate-free medium indicated that NHE-1 was activated (Cingolani *et al.* 1998). We also found that NHE-1 activation was suppressed by blockade of either AT1 or ETA receptors (Cingolani *et al.* 2005). This led us to propose that Ang II/ET were autocrine or paracrine mediators of this phenomenon (Cingolani *et al.* 1998). The NHE-1-mediated increase in intracellular Na^+ concentration (Perez *et al.* 2003), the increase in action potential duration (Zhou *et al.* 2006), and probably a redox-sensitive phosphorylation of the cardiac Na^+/Ca^{2+} exchanger (Eigel *et al.* 2004) appeared to be factors that contribute to the increase in contractility that follows myocardial stretch. Interestingly, in previous works, we were able to eliminate changes in pH_i as a possible contributor to the SFR (Alvarez *et al.* 1999; Perez *et al.* 2001), because under physiological conditions (bicarbonate buffer), the enhanced activity of NHE-1 was not accompanied by significant changes in pH_i. This was due to the simultaneous Ang II activation of the Na^+-independent Cl^-/HCO_3^- anion exchanger (Alvarez

et al. 2001; Cingolani *et al.* 2003). Several studies have shown that Ang II/ET increase ROS formation through a NADPH oxidase/mitochondrial action (Zorov *et al.* 2000; Seshiah *et al.* 2002; Cingolani *et al.* 2006). We recently proposed that the same signalling pathway plays a pivotal role in the genesis of the SFR to stretch (Caldiz *et al.* 2007) by activation of redox-sensitive kinases upstream of the NHE-1.

It has recently been established that transactivation of the EGFR is the primary mechanism that underlies GPCR agonist activation of ERK1/2 and its downstream intracellular pathways (Lemarie *et al.* 2008). Furthermore, myocardial stretch (Anderson *et al.* 2004; Duquesnes *et al.* 2009), myocardial hypertrophy (Kagiyama *et al.* 2002), and ET-1 signalling (Asakura *et al.* 2002) have been shown to involve EGFR transactivation. The present study has provided the first evidence for the crucial role of EGFR transactivation in the development of the SFR. Based on our previous and present findings, we propose that the hypothetical signalling pathway schematised in Fig. 9 is the mechanism that underlies SFR development. We have recently proposed a crucial role of mitochondrial ROS in promoting the development of the SFR (Caldiz *et al.* 2007); and the present work provides conclusive evidence that EGFR transactivation is a key step in the induction of mitochondrial ROS formation.

In addition, our experimental data clearly indicated that ROS signalling takes place downstream of mitochondrial stimulation, and upstream of ERK1/2 stimulation. However, this study did not rule out any additional effects that ROS might have had on one or several other reactions in the chain of events described in Fig. 9.
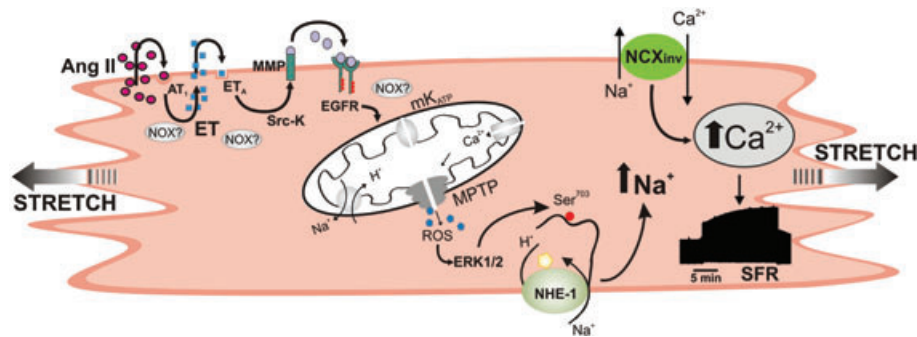

Figure 9. Scheme of the proposed mechanism leading to the SFR
Stretch and/or angiotensin II (Ang II) through AT1 receptor stimulation triggers the release/formation of endothelin (ET). NADPH oxidase-generated reactive oxygen species (ROS) probably play a significant role in this step of the signalling cascade. ET activates the ETA receptor and induces epidermal growth factor receptor (EGFR) transactivation. The communication between the ETA receptor and the EGFR involves matrix metalloprotease (MMP) activation and possibly the ROS-sensitive Src kinase. EGFR activation triggers an intracellular signalling pathway that leads to mKATP channel opening increasing ROS production and release through the mitochondrial permeability transition pore (MPTP). This causes ERK1/2 activation and NHE-1 phosphorylation at Ser703, increasing NHE-1 activity and intracellular Na^+ concentration that favours intracellular Ca^{2+} accumulation through the Na^+/Ca^{2+} exchanger (NCX). The increase in ROS production can also contribute to the increase in intracellular Ca^{2+} through a direct stimulatory effect on the NCX (Eigel *et al.* 2004) and by increasing action potential duration (Zhou *et al.* 2006).

For example, others have implicated ROS mediation in signalling pathways that lead to stretch-induced ET release (Anderson *et al.* 2004), kinase-dependent NHE-1 activation (Rothstein *et al.* 2002; Seshiah *et al.* 2002; Caldiz *et al.* 2007), MMP activation (Wetzker & Bohmer, 2003), and EGFR phosphorylation by inactivation of a phosphatase (Salmeen *et al.* 2003; van Montfort *et al.* 2003). ROS were also proposed to mediate the opening of mKATP channels through a NADPH oxidase-dependent mechanism that subsequently induced mitochondrial ROS release (Brandes, 2005; Kimura *et al.* 2005). It is also important to highlight that NADPH oxidase is now recognized to exist in different subcellular localisations that enable the targeting of specific compartments. In this context, it was difficult to determine, with the methods used in this study, the precise steps in which ROS were critically important in the chain of events triggered by stretch. However, we presented evidence that EGFR trans-activation is a crucial step in the ROS generation that leads to the Anrep effect.

References

Akram S, Teong HF, Fliegel L, Pervaiz S & Clement MV (2006). Reactive oxygen species-mediated regulation of the Na^+-H^+ exchanger 1 gene expression connects intracellular redox status with cells' sensitivity to death triggers. *Cell Death Differ* **13**, 628–641.

Alvarez BV, Fujinaga J & Casey JR (2001). Molecular basis for angiotensin II-induced increase of chloride/bicarbonate exchange in the myocardium. *Circ Res* **89**, 1246–1253.

Alvarez BV, Perez NG, Ennis IL, Camilion de Hurtado MC & Cingolani HE (1999). Mechanisms underlying the increase in force and Ca^{2+} transient that follow stretch of cardiac muscle: a possible explanation of the Anrep effect. *Circ Res* **85**, 716–722.

Allen DG & Kurihara S (1982). The effects of muscle length on intracellular calcium transients in mammalian cardiac muscle. *J Physiol* **327**, 79–94.

Anderson HD, Wang F & Gardner DG (2004). Role of the epidermal growth factor receptor in signalling strain-dependent activation of the brain natriuretic peptide gene. *J Biol Chem* **279**, 9287–9297.

Asakura M, Kitakaze M, Takashima S, Liao Y, Ishikura F, Yoshinaka T, Ohmoto H, Node K, Yoshino K, Ishiguro H, Asanuma H, Sanada S, Matsumura Y, Takeda H, Beppu S, Tada M, Hori M & Higashiyama S (2002). Cardiac hypertrophy is inhibited by antagonism of ADAM12 processing of HB-EGF: metalloproteinase inhibitors as a new therapy. *Nat Med* **8**, 35–40.

Brandes RP (2005). Triggering mitochondrial radical release: a new function for NADPH oxidases. *Hypertension* **45**, 847–848.

Calaghan SC & White E (2001). Contribution of angiotensin II, endothelin 1 and the endothelium to the slow inotropic response to stretch in ferret papillary muscle. *Pflugers Arch* **441**, 514–520.

Caldiz CI, Garciarena CD, Dulce RA, Novaretto LP, Yeves AM, Ennis IL, Cingolani HE, Chiappe de Cingolani G & Perez NG (2007). Mitochondrial reactive oxygen species activate the slow force response to stretch in feline myocardium. *J Physiol* **584**, 895–905.

Cingolani HE, Alvarez BV, Ennis IL & Camilion de Hurtado MC (1998). Stretch-induced alkalinization of feline papillary muscle: an autocrine-paracrine system. *Circ Res* **83**, 775–780.

Cingolani HE, Chiappe GE, Ennis IL, Morgan PG, Alvarez BV, Casey JR, Dulce RA, Perez NG & Camilion de Hurtado MC (2003). Influence of Na^+-independent Cl^--HCO_3^- exchange on the slow force response to myocardial stretch. *Circ Res* **93**, 1082–1088.

Cingolani HE, Perez NG, Aiello EA & de Hurtado MC (2005). Intracellular signalling following myocardial stretch: an autocrine/paracrine loop. *Regul Pept* **128**, 211–220.

Cingolani HE, Villa-Abrille MC, Cornelli M, Nolly A, Ennis IL, Garciarena C, Suburo AM, Torbidoni V, Correa MV, Camilion de Hurtado MC & Aiello EA (2006). The positive inotropic effect of angiotensin II: role of endothelin-1 and reactive oxygen species. *Hypertension* **47**, 727–734.

Dikalov S, Griendling KK & Harrison DG (2007). Measurement of reactive oxygen species in cardiovascular studies. *Hypertension* **49**, 717–727.

Drummond GB (2009). Reporting ethical matters in *The Journal of Physiology*: standards and advice. *J Physiol* **587**, 713–719.

Duquesnes N, Vincent F, Morel E, Lezoualc'h F & Crozatier B (2009). The EGF receptor activates ERK but not JNK Ras-dependently in basal conditions but ERK and JNK activation pathways are predominantly Ras-independent during cardiomyocyte stretch. *Int J Biochem Cell Biol* **41**, 1173–1181.

Eigel BN, Gursahani H & Hadley RW (2004). ROS are required for rapid reactivation of Na^+/Ca^{2+} exchanger in hypoxic reoxygenated guinea pig ventricular myocytes. *Am J Physiol Heart Circ Physiol* **286**, H955–963.

Ennis IL, Cingolani HE, Garciarena CD, Camilión de Hurtado MC, Villa-Abrille MC, Aiello EA & Pérez NG (2007). From Anrep's Phenomenon to myocardial hypertrophy: Role of the Na^+/H^+ exchanger. *Curr Cardiol Rev* **3**, 149–164.

Fliegel L & Karmazyn M (2004). The cardiac Na-H exchanger: a key downstream mediator for the cellular hypertrophic effects of paracrine, autocrine and hormonal factors. *Biochem Cell Biol* **82**, 626–635.

Haworth RS, McCann C, Snabaitis AK, Roberts NA & Avkiran M (2003). Stimulation of the plasma membrane Na^+/H^+ exchanger NHE1 by sustained intracellular acidosis. Evidence for a novel mechanism mediated by the ERK pathway. *J Biol Chem* **278**, 31676–31684.

Ito H, Hirata Y, Adachi S, Tanaka M, Tsujino M, Koike A, Nogami A, Murumo F & Hiroe M (1993). Endothelin-1 is an autocrine/paracrine factor in the mechanism of angiotensin II-induced hypertrophy in cultured rat cardiomyocytes. *J Clin Invest* **92**, 398–403.

Kagiyama S, Eguchi S, Frank GD, Inagami T, Zhang YC & Phillips MI (2002). Angiotensin II-induced cardiac hypertrophy and hypertension are attenuated by epidermal growth factor receptor antisense. *Circulation* **106**, 909–912.

Kentish JC & Wrzosek A (1998). Changes in force and cytosolic Ca^{2+} concentration after length changes in isolated rat ventricular trabeculae. *J Physiol* **506**, 431–444.

Kimura S, Zhang GX, Nishiyama A, Shokoji T, Yao L, Fan YY, Rahman M, Suzuki T, Maeta H & Abe Y (2005). Role of NAD(P)H oxidase- and mitochondria-derived reactive oxygen species in cardioprotection of ischemic reperfusion injury by angiotensin II. *Hypertension* **45**, 860–866.

Krieg T, Cui L, Qin Q, Cohen MV & Downey JM (2004). Mitochondrial ROS generation following acetylcholine-induced EGF receptor transactivation requires metalloproteinase cleavage of proHB-EGF. *J Mol Cell Cardiol* **36**, 435–443.

Lehoux S, Abe J, Florian JA & Berk BC (2001). 14-3-3 Binding to Na^+/H^+ exchanger isoform-1 is associated with serum-dependent activation of Na^+/H^+ exchange. *J Biol Chem* **276**, 15794–15800.

Lemarie CA, Paradis P & Schiffrin EL (2008). New insights on signalling cascades induced by cross-talk between angiotensin II and aldosterone. *J Mol Med* **86**, 673–678.

Leri A, Claudio PP, Li Q, Wang X, Reiss K, Wang S, Malhotra A, Kajstura J & Anversa P (1998). Stretch-mediated release of angiotensin II induces myocyte apoptosis by activating p53 that enhances the local renin-angiotensin system and decreases the Bcl-2-to-Bax protein ratio in the cell. *J Clin Invest* **101**, 1326–1342.

Luers C, Fialka F, Elgner A, Zhu D, Kockskamper J, von Lewinski D & Pieske B (2005). Stretch-dependent modulation of $[Na^+]_i$, $[Ca^{2+}]_i$, and pH_i in rabbit myocardium: a mechanism for the slow force response. *Cardiovasc Res* **68**, 454–463.

Monroe RG, Gamble WJ, LaFarge CG, Kumar AE, Stark J, Sanders GL, Phornphutkul C & Davis M (1972). The Anrep effect reconsidered. *J Clin Invest* **51**, 2573–2583.

Parmley WW & Chuck L (1973). Length-dependent changes in myocardial contractile state. *Am J Physiol* **224**, 1195–1199.

Perez NG, Caldiz CI, Chiappe de Cingolani GE & Cingolani HE (2009). The slow force response to myocardial stretch requires transactivation of the epidermal growth factor receptor. *Circulation* **120**, S782–S783.

Perez NG, de Hurtado MC & Cingolani HE (2001). Reverse mode of the Na^+-Ca^{2+} exchange after myocardial stretch: underlying mechanism of the slow force response. *Circ Res* **88**, 376–382.

Perez NG, Villa-Abrille MC, Aiello EA, Dulce RA, Cingolani HE & Camilion de Hurtado MC (2003). A low dose of angiotensin II increases inotropism through activation of reverse Na^+/Ca^{2+} exchange by endothelin release. *Cardiovasc Res* **60**, 589–597.

Rosenblueth A, Alanis J, Lopez E & Rubio R (1959). The adaptation of ventricular muscle to different circulatory conditions. *Arch Int Physiol Biochem* **67**, 358–373.

Rothstein EC, Byron KL, Reed RE, Fliegel L & Lucchesi PA (2002). H_2O_2-induced Ca^{2+} overload in NRVM involves ERK1/2 MAP kinases: role for an NHE-1-dependent pathway. *Am J Physiol Heart Circ Physiol* **283**, H598–605.

Sabri A, Byron KL, Samarel AM, Bell J & Lucchesi PA (1998). Hydrogen peroxide activates mitogen-activated protein kinases and Na^+-H^+ exchange in neonatal rat cardiac myocytes. *Circ Res* **82**, 1053–1062.

Sadoshima J, Xu Y, Slayter HS & Izumo S (1993). Autocrine release of angiotensin II mediates stretch-induced hypertrophy of cardiac myocytes in vitro. *Cell* **75**, 977–984.

Salmeen A, Andersen JN, Myers MP, Meng TC, Hinks JA, Tonks NK & Barford D (2003). Redox regulation of protein tyrosine phosphatase 1B involves a sulphenyl-amide intermediate. *Nature* **423**, 769–773.

Sarnoff SJ, Mitchell JH, Gilmore JP & Remensnyder JP (1960). Homeometric autoregulation in the heart. *Circ Res* **8**, 1077–1091.

Seshiah PN, Weber DS, Rocic P, Valppu L, Taniyama Y & Griendling KK (2002). Angiotensin II stimulation of NAD(P)H oxidase activity: upstream mediators. *Circ Res* **91**, 406–413.

Snabaitis AK, D'Mello R, Dashnyam S & Avkiran M (2006). A novel role for protein phosphatase 2A in receptor-mediated regulation of the cardiac sarcolemmal Na^+/H^+ exchanger NHE1. *J Biol Chem* **281**, 20252–20262.

Szokodi I, Kerkela R, Kubin AM, Sarman B, Pikkarainen S, Konyi A, Horvath IG, Papp L, Toth M, Skoumal R & Ruskoaho H (2008). Functionally opposing roles of extracellular signal-regulated kinase 1/2 and p38 mitogen-activated protein kinase in the regulation of cardiac contractility. *Circulation* **118**, 1651–1658.

Takahashi E, Abe J, Gallis B, Aebersold R, Spring DJ, Krebs EG & Berk BC (1999). p90(RSK) is a serum-stimulated Na^+/H^+ exchanger isoform-1 kinase. Regulatory phosphorylation of serine 703 of Na^+/H^+ exchanger isoform-1. *J Biol Chem* **274**, 20206–20214.

van Montfort RL, Congreve M, Tisi D, Carr R & Jhoti H (2003). Oxidation state of the active-site cysteine in protein tyrosine phosphatase 1B. *Nature* **423**, 773–777.

von Anrep G (1912). On the part played by the suprarenals in the normal vascular reactions on the body. *J Physiol* **45**, 307–317.

Wetzker R & Bohmer FD (2003). Transactivation joins multiple tracks to the ERK/MAPK cascade. *Nat Rev Mol Cell Biol* **4**, 651–657.

Yamazaki T, Komuro I, Kudoh S, Zou Y, Nagai R, Aikawa R, Uozumi H & Yazaki Y (1998). Role of ion channels and exchangers in mechanical stretch-induced cardiomyocyte hypertrophy. *Circ Res* **82**, 430–437.

Yamazaki T, Komuro I, Kudoh S, Zou Y, Shiojima I, Hiroi Y, Mizuno T, Maemura K, Kurihara H, Aikawa R, Takano H & Yazaki Y (1996). Endothelin-1 is involved in mechanical stress-induced cardiomyocyte hypertrophy. *J Biol Chem* **271**, 3221–3228.

Zhai P, Galeotti J, Liu J, Holle E, Yu X, Wagner T & Sadoshima J (2006). An angiotensin II type 1 receptor mutant lacking epidermal growth factor receptor transactivation does not induce angiotensin II-mediated cardiac hypertrophy. *Circ Res* **99**, 528–536.

Zhang YH, Dingle L, Hall R & Casadei B (2009). The role of nitric oxide and reactive oxygen species in the positive inotropic response to mechanical stretch in the mammalian myocardium. *Biochim Biophys Acta* **1787**, 811–817.

Zhou C, Ziegler C, Birder LA, Stewart AF & Levitan ES (2006). Angiotensin II and stretch activate NADPH oxidase to destabilize cardiac Kv4.3 channel mRNA. *Circ Res* **98**, 1040–1047.

Zorov DB, Filburn CR, Klotz LO, Zweier JL & Sollott SJ (2000). Reactive oxygen species (ROS)-induced ROS release: a new phenomenon accompanying induction of the mitochondrial permeability transition in cardiac myocytes. *J Exp Med* **192**, 1001–1014.

Author contributions

M.C.V.A., H.E.C. and N.G.P.: conception and design of the experiments, collection, analysis and interpretation of data, drafting the article and revising it critically for important intellectual content. M.B.N., M.J.C. and C.I.C.: collection, analysis and interpretation of data. I.L.E. and G.E.C.de C.: conception and design of the experiments, drafting the article and revising it critically for important intellectual content. All authors have read and approved the final version of the manuscript.

Acknowledgements